Available online at www.eccomasproceedia.org
Eccomas Proceedia COMPDYN (2025) 1862-1869

ECCOMAS
Proceedia

COMPDYN 2025
10th ECCOMAS Thematic Conference on
Computational Methods in Structural Dynamics and Earthquake Engineering
M. Papadrakakis, M. Fragiadakis (eds.)
Rhodes Island, Greece, 15-18 June 2025

A NUMERICAL INVESTIGATION ON THE RATE DEPENDENCE OF LEAD EXTRUSION DAMPERS

Furkan Çalım[1], Ahmet Güllü[1*], Cihan Soydan[2], and Ercan Yüksel[1]

[1] Faculty of Civil Engineering, Istanbul Technical University
Maslak, 34469 Sariyer, Istanbul, Türkiye
calimf@itu.edu.tr, ahmetgullu@itu.edu.tr, yukselerc@itu.edu.tr

[2] Department of Civil Engineering, Tekirdag Namik Kemal University
59030 Suleymanpasa, Tekirdag, Türkiye
csoydan@nku.edu.tr

Abstract

Lead extrusion damper is a highly effective energy dissipation device widely used in seismic mitigation systems. By forcing lead to flow through a restricted orifice formed by a bulged shaft at its core, this damper provides high energy dissipation capacity while maintaining a compact design. In the literature studies, some argue that the lead extrusion dampers are rate-dependent, while others suggest that the effects of loading rates are negligible. This study investigates the rate-dependent behavior of lead extrusion dampers through a set of finite element analyses conducted in ABAQUS software. An experimentally validated numerical model simulates damper performance under various loading rates. The effects of varying loading rates on the damper force and energy dissipation capacity are systematically evaluated. After discussing the success of some velocity models suggested in the literature, further refinements are proposed to enhance their precision.

Keywords: Finite Element Analysis, Lead Extrusion Damper, HF2V Damper, Passive Energy Dissipater, Seismic Energy Dissipation.

ISSN:2623-3347
Peer-review under responsibility of the organizing committee of COMPDYN 2025.
doi: 10.7712/120125.12534.25951

1 INTRODUCTION

Seismic energy dissipation devices play a crucial role in enhancing the performance of structures under earthquake excitations. Among various types of energy dissipation devices employing passive energy dissipation systems, lead extrusion dampers (LEDs), which were originally developed in the mid-1970s [1-2], have gained significant attention due to their high energy dissipation capacity, stable hysteretic behavior, and ease of implementation in both new and retrofitted structures [3].

Although extensive research has been conducted on the development and performance enhancement of LEDs, their rate dependence remains a subject of debate. While some studies highlight a significant influence of loading rates, others suggest their effects are negligible. Robinson and Greenbank [1] experimentally investigated the rate dependence of LEDs across a range from 2×10^{-7} mm/s to 600 mm/s. They identified a threshold loading rate of 0.017 mm/s, below which a tenfold increase in the loading rate resulted in a 32% increase in the damper force, while above this threshold, the increase was only 7%. Their findings suggest that LEDs exhibit significant rate dependence at lower loading rates but become nearly velocity-independent at relatively higher rates. They also proposed an empirical relationship between extrusion force (F) and loading rate (v), where the coefficient b was defined as 0.12 for loading rates below the threshold and 0.03 for the ones above the threshold, as displayed in Equation (1) [2]. Cousins and Porritt [4] later argued that this coefficient should be suggested based on damper type, with values of 0.12 for bulged shaft LEDs and 0.03 for constricted tube LEDs. Rodgers [5] supported this classification, reporting similar values for bulged shaft LEDs tested under loading rates up to 1.0 mm/s. Golondrino et al. [6-7] claimed that the aforementioned formulation successfully represents the relationship between loading rate and damper force, yet by employing different b coefficients. Tsai et al. [8] further expanded on this by incorporating temperature effects into the force-loading rate relationship, accounting for heat generation from plastic deformation, as formulated in Equation (2).

$$F(t) = a \cdot v^b(t) \tag{1}$$

$$F(t) = \alpha \cdot \left(1 + \gamma \cdot e^{-\beta \cdot \left\lfloor \int F(t) \cdot du(t) + \theta \cdot (T - T_0) \right\rfloor} \right) \cdot v^b(t) \tag{2}$$

Conversely, a contrasting viewpoint suggests that the damper force is independent of the loading rate. Parulekar et al. [9] claimed that extrusion force depends solely on the device's geometry (i.e., bulge angle, cross-sectional and extruded area of the lead, stroke length, and shaft diameter) and material properties (i.e., lead's yield strength and friction), rather than the loading rate. Rodgers et al. [10] supported this argument by testing LEDs under loading rates ranging from 2.5 mm/s to 200 mm/s, finding that although extrusion force increased with the loading rate, frictional resistance decreased. The opposing effects of increasing extrusion resistance and decreasing frictional resistance resulted in nearly constant damper force, suggesting that LEDs operate independently of the loading rate at higher velocities.

Given the ongoing debate on the rate dependence of LEDs and the varying conclusions drawn from previous literature studies, it is essential to further investigate this phenomenon to provide a more comprehensive understanding. This study aims to numerically investigate the rate dependence of bulged-shaft type LEDs using an experimentally validated finite element modeling strategy. The primary objectives are to compare numerical predictions with available experimental data, evaluate the influence of different loading rates on the damper force and energy dissipation capacity, and provide insights into the loading rate sensitivity of lead inside the dampers.

2 LEAD EXTRUSION DAMPER

The LED comprises three main components, i.e., a shaft, an outer tube, and lead filled between them. The constriction for the lead's extrusion process was formed through a spherical bulge at the mid-section of the shaft. The damper used in this study was selected from those previously developed by the authors [11]. Specifically, the device labeled *B44-L100-R00-P1.5* in that study was utilized, as displayed in Figure 1. The bulge and shaft diameters of this specific device are 44 mm and 32 mm, respectively, while the outer tube has an inner radius of 60 mm and a thickness of 12 mm. The minimum clearance between the bulge and the inner surface of the tube is 8 mm. Once the shaft is positioned, the tube is filled with lead to complete the damper assembly. The damper provides a displacement capacity of ±33 mm when the bulge is centered at mid-stroke.

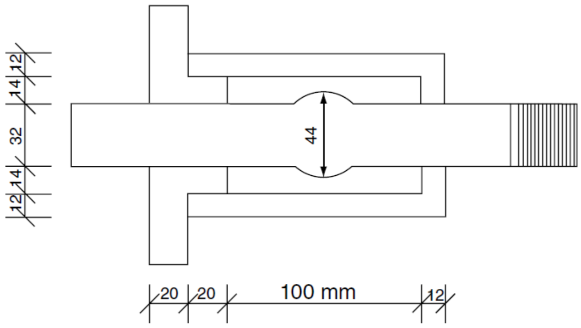

(a) Geometric dimensions

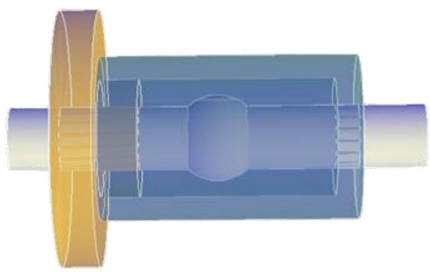

(b) 3D view

Figure 1: Properties of the investigated LED.

The experimental study for the performance evaluation of the investigated LED was conducted under three reversal cyclic steps (i.e., ±5 mm displacement target at 0.5 mm/s rate, ±10 mm displacement target at 1.0 mm/s rate, and ±20 mm displacement target at 2.0 mm/s rate) [11]. The hysteretic behavior of the investigated LED obtained as a result of the cyclic loading steps is presented in Figure 2. It reached a maximum damper force of around 215 kN, 280 kN, and 300 kN in the ±5 mm, ±10 mm, and ±20 mm steps, respectively. This device resulted in an almost rectangular hysteresis with a trailing void length of around 10 mm in the last step of the loading protocol.

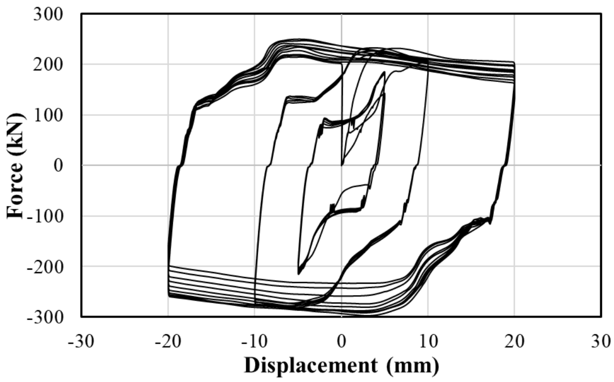

Figure 2: Hysteretic behavior of the investigated LED.

3 FINITE ELEMENT MODELING STRATEGY

Three-dimensional finite element models for the LEDs were generated utilizing the *ABAQUS* finite element analysis software. To improve the accuracy of the analyses, detailed models were developed using the exact element geometry and actual material test results.

3.1 Material properties

The bulged shaft and outer tube of the damper are manufactured utilizing CK45-type steel, i.e., ISO-equivalent grade of C45E4 and ASTM-equivalent grade of 1045). The material properties of the lead and CK45-type steel used in the damper were previously determined by Çalım et al. [12] through standard tensile tests. While the yield and maximum strength values were experimentally obtained as 9 MPa and 20 MPa for the lead, they were 410 MPa and 680 MPa for the CK45-type steel, respectively.

In the finite element models, a combined isotropic/kinematic hardening model was chosen to represent the inelastic behavior of the materials because it accurately predicts the response of metals under cyclic loading, accounting for effects like ratcheting and cyclic hardening. For the kinematic hardening part of the model, the “Half Cycle” option was used to input stress-strain data from the first half of the unidirectional tensile tests. The engineering stress-strain curves from these tests were converted into true stress-strain curves using Equations (3) and (4) to define the inelastic material properties in the models, as displayed in Figure 3.

$$\sigma_{true} = \sigma_{engineering} \cdot (1 + \varepsilon_{engineering}) \tag{3}$$

$$\varepsilon_{true} = \ln(1 + \varepsilon_{engineering}) \tag{4}$$

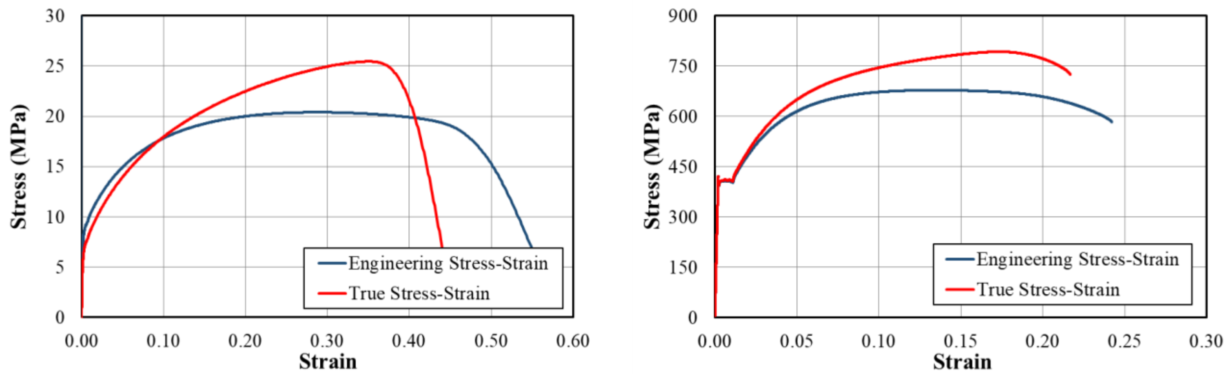

(a) Lead (b) Steel

Figure 3: Engineering and true stress-strain relationships employed in the finite element models.

3.2 Interaction definitions

Solid and homogenous sections were assigned to each component modeled as three-dimensional deformable parts, employing the predefined material properties. Standard surface-to-surface contact interaction was defined to represent the interaction between the steel and lead surfaces. A penalty-type friction formulation with a friction coefficient of 0.25 was utilized for tangential behavior, whereas the hard contact pressure-overclosure relationship was selected for the normal behavior.

3.3 Finite element meshing

Eight-node linear brick elements with reduced integration and hourglass control (C3D8R), which are well-suited for simulations involving large deformations and nonlinear material behavior, were utilized for the finite element meshing of the modeled parts, as displayed in Figure 4. They were specifically chosen to ensure a balance between computational efficiency and numerical stability, enabling accurate modeling of the large plastic deformations in LEDs. The meshing element size was chosen considering both the accuracy of the model and the computational time. The applied fine meshing resulted in a total of 39440 C3D8R-type finite elements (i.e., 4800 elements on the cylinder, 13440 elements on the shaft, and 21200 elements on the lead).

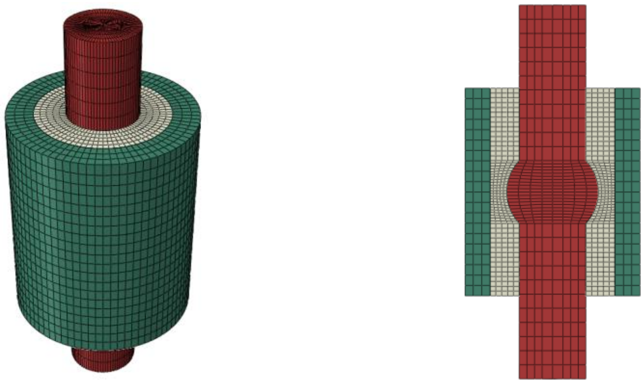

(a) 3D view (b) Section view

Figure 4: Finite element meshing of LEDs.

In the finite element models, Arbitrary Lagrangian-Eulerian (ALE) adaptive meshing was employed to enhance the numerical stability of the analysis by redistributing mesh nodes without altering element connectivity. The frequency of adaptive meshing was set to five, meaning that remeshing was performed every five increments. This setting strikes a balance between computational efficiency and mesh quality preservation, as more frequent remeshing would increase computational cost, while less frequent remeshing could lead to element deterioration. Additionally, three remeshing sweeps per increment were specified, ensuring that the mesh was smoothed adequately before the next increment proceeded. This approach prevents excessive mesh distortion and enhances numerical accuracy while maintaining a reasonable computational demand.

3.4 Loading protocol

A dynamic analysis step was defined to simulate LEDs' response under cyclic loading. A velocity-controlled loading protocol was applied to the top of the bulged shaft, where the damper was subjected to a cyclic loading sequence with an amplitude of ±5 mm. On the other hand, the damper's movement was restricted by assigning "encastre" (fixed) boundary conditions at the bottom surface of the outer tube. To verify the accuracy of the generated finite element model, an initial analysis was conducted using a loading rate of 0.5 mm/s, ensuring comparability with the experimental study. Subsequently, to examine the rate dependence of LEDs, additional simulations were performed at varying loading rates to allow for an assessment of viscoplastic effects, as lead exhibits strain-rate sensitivity that influences both force resistance and energy dissipation capacity.

Notably, the effects of nonlinearity caused by both the material and geometry were considered in the analyses.

4 INVESTIGATION ON THE RATE DEPENDENCE

First, the generated benchmark finite element model was validated utilizing the experimentally obtained force-displacement hysteresis curve [11]. Specifically, the numerical hysteresis response was evaluated against the first cyclic step of the experimental program, which involved a ±5 mm displacement target at a loading rate of 0.5 mm/s. The comparison revealed a strong agreement in terms of damper forces and loading/unloading paths, confirming the model's ability to replicate the experimental behavior. However, minor fluctuations were observed in the numerical force-displacement hysteresis curve, likely due to numerical artifacts or local instabilities in the simulation. To enhance clarity and improve interpretability, a smoothing process was applied to the numerical curve, Figure 5.

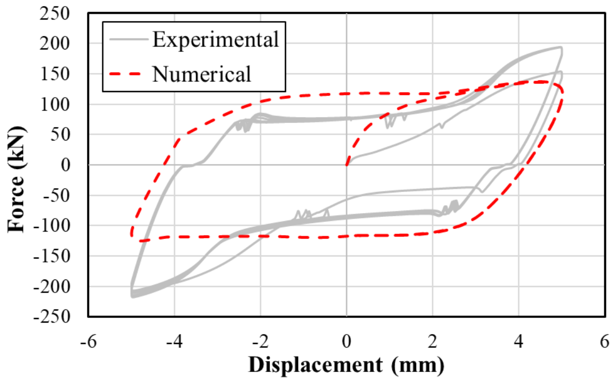

Figure 5: Experimental validation of the benchmark finite element model.

The rate-dependent behavior of the LED was investigated by simulating the damper's response under loading rates ranging from 0.001 mm/s to 10 mm/s. Figure 6 illustrates the variation in damper force with varying loading rates. The results indicate that the damper force increases with the loading rate.

However, the rate of increase differs below and above a threshold loading rate level of 0.05 mm/s. Specifically, for loading rates below this threshold, the force exhibits a more pronounced increase. This suggests that the LED is relatively more sensitive to loading rates at lower velocities, where the viscoplastic behavior of lead dominates the response. The increase in force is attributed to the strain-rate sensitivity of lead, which results in higher resistance to extrusion at lower loading rates.

On the other hand, the increase becomes more gradual beyond this threshold. This indicates that the LED becomes less sensitive to loading rates at higher velocities, approaching a nearly rate-independent behavior. This phenomenon can be explained by the balance between the increasing extrusion resistance and the decreasing frictional resistance at higher loading rates.

To compute the damper force with respect to the loading rate, Equation (5) was suggested. Here, F is the maximum damper force, v is the loading rate, and F_t is the maximum damper force at the threshold loading rate level (i.e., 132 kN for the studied LED geometry).

$$F = \begin{cases} F_t \cdot (20 \cdot v)^{0.07} & v \leq 0.05 \; mm/s \\ F_t \cdot (20 \cdot v)^{0.02} & v > 0.05 \; mm/s \end{cases} \tag{5}$$

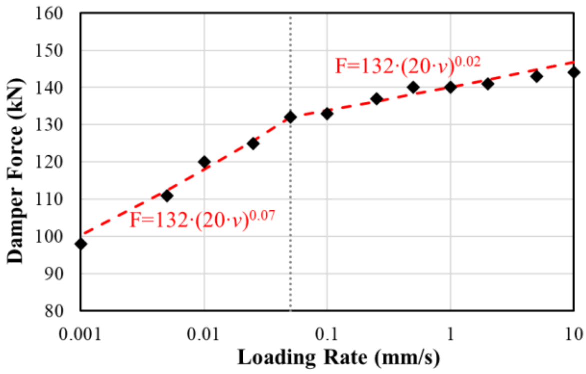

Figure 6: Change in the damper force with respect to the loading rate.

5 CONCLUSIONS

This study investigated the rate-dependent behavior of lead extrusion dampers (LEDs) through a series of finite element analyses. The numerical benchmark model was validated against experimental data, demonstrating its ability to accurately replicate the hysteretic behavior of the LED. As a result, the following conclusions could be driven:

- The results support the argument that LEDs exhibit rate-dependent behavior, particularly at lower loading rates. The results are consistent with the observations in the previous literature studies, which identified a threshold loading rate below which the damper force increases significantly with the loading rate. Above this threshold, the damper force becomes less sensitive to loading rates, suggesting that the LED operates in a nearly rate-independent manner at higher velocities.
- The proposed equation provides a simple yet effective way to predict the damper force as a function of the loading rate. The inclusion of a threshold loading rate and rate-dependent coefficients allows for a more accurate representation of the LED's behavior across a wide range of loading conditions. Different from the literature studies, the threshold value was defined as 0.05 mm/s. In addition, new coefficients were employed in proposing this equation.
- The findings of this study have important implications for the design and implementation of LEDs for structural response control. By understanding the rate-dependent behavior of these devices, one can optimize their performance and ensure their effectiveness in mitigating the effects of earthquakes.

This study contributes to the ongoing debate on LEDs' rate dependence by providing an experimentally validated finite element framework for analyzing their behavior under varying loading rates. The proposed equation, along with the defined loading rate threshold and new coefficients, offers a refined approach to predicting damper forces.

ACKNOWLEDGMENTS

This study has been supported by TÜBİTAK (The Scientific and Technological Research Council of Türkiye) within the scope of the 2224-A International Scientific Events Participation Support Program.

REFERENCES

[1] W.H. Robinson, L.R. Greenbank, Properties of an extrusion energy absorber. *Bulletin of the New Zealand Society for Earthquake Engineering*, **8(3)**, 187-191, 1975. https://doi.org/10.5459/bnzsee.8.3.187-191

[2] W.H. Robinson, L.R. Greenbank, An extrusion energy absorber suitable for the protection of structures during an earthquake. *Earthquake Engineering and Structural Dynamics*, **4(3)**, 251–259, 1976. https://doi.org/10.1002/eqe.4290040306

[3] F. Çalım, A. Güllü, C. Soydan, E. Yüksel, State-of-the-art review for lead extrusion dampers: Development, improvement, characteristics, application areas, and research needs. *Structures*, **58**, 105477, 2023. https://doi.org/10.1016/j.istruc.2023.105477

[4] W.J. Cousins, T.E. Porritt, Improvements to lead-extrusion damper technology. *Bulletin of the New Zealand Society for Earthquake Engineering*, **26(3)**, 342–348, 1993. https://doi.org/10.5459/bnzsee.26.3.342-348

[5] G.W. Rodgers, Next-generation structural technologies: Implementing high force-to-volume energy absorbers. Ph.D. Dissertation, *University of Canterbury*, Christchurch, New Zealand, 2009.

[6] J.C. Golondrino, G. Chase, G.W. Rodgers, G.A. MacRae, C. Clifton, Velocity effects on the behaviour of high-force-to-volume lead dampers (HF2V) using different shaft configurations. *15th World Conference on Earthquake Engineering*. Lisboa, Portugal, 2012.

[7] J.C. Golondrino, G. Chase, G.W. Rodgers, G.A. MacRae, C. Clifton, Velocity dependence of HF2V devices using different shaft configurations. *2012 New Zealand Society for Earthquake Engineering Annual Conference*. Napier, New Zealand, 2012.

[8] C.S. Tsai, W.S. Lai, C.W. Chang, M.C. Li, Testing and analysis of a new lead-extrusion damper. *Pressure Vessels and Piping Conference*, Vancouver, Canada, 2002. https://doi.org/10.1115/pvp2002-1419

[9] Y.M. Parulekar, G.R. Reddy, K.K. Vaze, H.S. Kushwaha, Lead extrusion dampers for reducing seismic response of coolant channel assembly. *Nuclear Engineering and Design*, **227(2)**, 175-183, 2004. https://doi.org/10.1016/j.nucengdes.2003.09.006

[10] G.W. Rodgers, G. Chase, D. Heaton, L. Cleeve, Testing of lead extrusion damping devices undergoing representative earthquake velocities. *2013 New Zealand Society for Earthquake Engineering Annual Conference*. Napier, New Zealand, 2013.

[11] C. Soydan, F. Çalım, A. Güllü, E. Yüksel, Experimental investigation of the effective parameters on the lead extrusion damper performance. *Engineering Structures*, **318**, 118714, 2024. https://doi.org/10.1016/j.engstruct.2024.118714

[12] F. Çalım, A. Güllü, C. Soydan, E. Yüksel, Development and experimental validation of finite element models for a prestressed lead extrusion damper. *Structures*, **50**, 1114-1125, 2023. http://doi.org/10.1016/j.istruc.2023.02.094